

## Concept for spectrally resolved ITER divertor thermography with fibres

R.Reichle<sup>1</sup>, S. Henry<sup>2</sup>, J.B. Migozzi<sup>3</sup>, E. Thomas<sup>1</sup>, C. Walker<sup>4</sup>

<sup>1</sup> Ass. EURATOM-CEA, DSM/DRFC, CEA-Cadarache, 13108 St. Paul-lez-Durance, France

<sup>2</sup> EISTI, 95011 Cergy, France

<sup>3</sup> JBM Optique, 11 avenue de la division Leclerc, 92310 SEVRES, France

<sup>4</sup> ITER-IT, p/a Max-Planck IPP, Boltzmannstr. 2, 85748 Garching bei München, Germany

Infrared thermography on tokamak target plates under plasma impact performed at a single wavelength may be misleading because the temperature at the surface of a target is not homogeneous [1-3]. Since the existing ITER divertor thermography diagnostic proposal [4] did not include the possibility to measure at multiple wavelengths at one place, a study was performed to remedy this with a diagnostic proposal based on a fibre-optics approach.

We have found an inverse matrix method to deduce the distribution of the target temperature from the spectral radiance distribution that can be applied successfully to experimental data of Tore Supra (fig. 1). This method approximates the real temperature distribution by a set of well defined discrete temperatures  $T_n$  between 200 and 1800°C. The measured spectral radiance  $L_m$  is given at the  $m$  different wavelengths  $\lambda_m$  spanning the range that can be used at Tore Supra (1.3-2.3  $\mu\text{m}$  from silica fibres or 1.3-4  $\mu\text{m}$  from  $\text{ZrF}_4$  fibres with 12 or 30 points resolution) or ITER, which is at most 1-10 microns ( $\approx 30$  points assumed). The relation between these quantities can be described by a matrix operation  $P_{mn} \times S_n = L_m$ , where the matrix  $P_{mn}$  contains the spectral blackbody radiance for  $m$  wavelengths (in the rows) at  $n$  temperatures (in the columns). The aim is to determine the weight value distribution  $S_n$  that describes the fractions at which the temperatures  $T_n$  are present on the target. This is done with the operation  $S_n = ({}^tP_{nm} \times P_{mn})^{-1} \times {}^tP_{nm} \times L_m$ . The problem is the sensitivity to noise. For  $n$

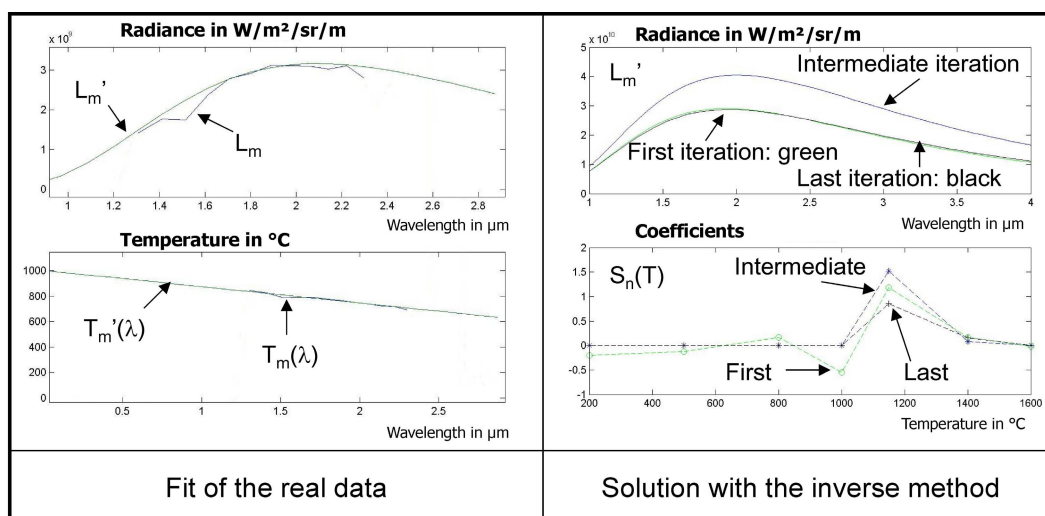


Fig. 1: Determination of a temperature distribution from a spectral radiance distribution.

= 7 and a spectral range of 1-10  $\mu\text{m}$  the method works with 1% noise on the input data. The spectral range in Tore Supra is 1.3-2.3  $\mu\text{m}$  with larger noise levels. We achieved nevertheless stable solutions by taking advantage of a peculiarity of the data: if one uses the measured spectral radiance data  $L_m(\lambda)$  to calculate at each wavelength  $\lambda_m$  a temperature  $T_m(\lambda)$  using the proper emissivity value  $\epsilon(\lambda)$  of the material, one finds that the  $T_m(\lambda)$  values decrease (nearly) linearly with increasing  $\lambda$ . By transformation of  $L_m$  into  $T_m$ , fitting a straight line to  $T_m$ , and thus finding the smoothed values  $T_m'$  and back-transforming them into  $L_m'$  values, one achieves virtually noise free data that can be treated by the inversion algorithm. The actual algorithm iterates to eliminate non-physical negative  $S_n$  values (fig. 1). The solutions seem to be robust against calibration errors and may allow to discriminate thermal radiation against the bremsstrahlung (compare with fig. 5) from the plasma.

Fibres are a natural choice for spectroscopic diagnostics. They minimise movements problems and they offer good possibilities for laser methods for calibration [5] and active measurements [6] as presumed necessary for an environment containing deposited layers and low emissivity, high reflection materials as tungsten and beryllium.

Due to the high environmental temperature of 150°C the choice of fibres is limited. The transmission of some of the most interesting fibre is summarized in fig. 2: low OH silica fibres (OE Oxford electronics), ZrF<sub>4</sub> fibres (IRG1, IRG2 Verre Fluoré and RA Reflex Analytical) and hollow wave guide fibres (HWCA, HWEA Polymicro). Sapphire fibres have transmission characteristics similar to

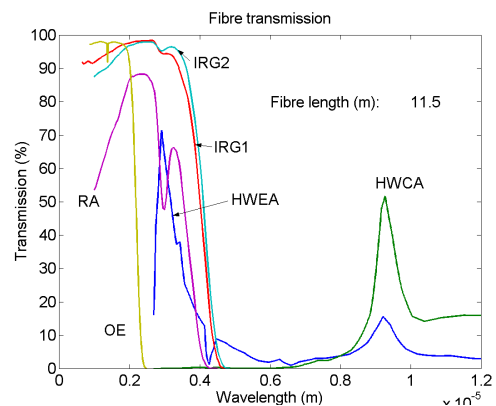


Fig. 2: Transmission of fibres.

ZrF<sub>4</sub> fibres but so far there is no good cladding available. An interesting potential future development that is here called Thermography Optimised Hollow Waveguide (TOHW) [7], is a coaxial combination of a hollow waveguide and a conventional fibre. It might allow to use the silica mantle to illuminate the target with near IR lasers and to measure with the hollow core the thermal excitation in the IR range. The present day silver coating of hollow fibres would have to be replaced – maybe by aluminium or rhodium.

The radiation environment in the divertor cassette is too hostile for fibres [8]. The region from the outboard side of the cassette along the divertor pumping duct to the bioshield shows an exponential radiation decay (decay length of 1.6 m) along this potential fibre path. The neutron dose rate for full power operation is about  $10^{13}$  n/cm<sup>2</sup>sec at the cassette and  $0.5 \cdot 10^{10}$

n/cm<sup>2</sup>sec in a distance of 8.6 m at the bioshield. The full lifetime dose of ITER (7600 hours) at the potential fibre connection point at the cassette (fig. 4) is about  $3 \cdot 10^{23}$  n/m<sup>2</sup>. Useful radiation darkening data were only found for silica fibres. Fig. 3 shows radiation induced attenuation data for a good silica fibre (KS4V) from JMTR [9] and SCK-CEN [10]. In the most optimistic interpretation of the data, fibres can be taken up to the cassette with 22% transmission (acceptance of 1dB/m of radiation darkening) remaining after the whole lifetime. In the most pessimistic interpretation an optical relay is necessary of 4.5 m for full lifetime operation or of 1.5 m if the fibres are exchanged every 1/8<sup>th</sup> of the full dose.

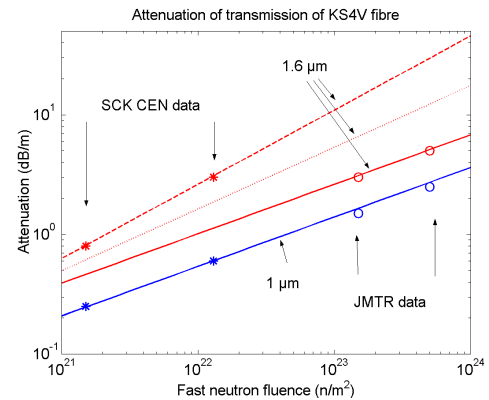


Fig. 3: Radiation induced attenuation.

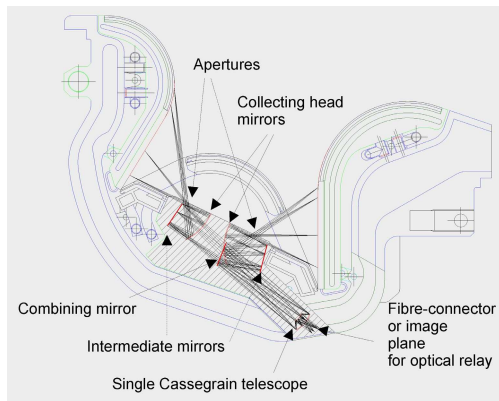


Fig. 4: Side view of front-end optic.

An optical study was performed to conceive an all-mirror optical front-end design suitable to a fibre solution (fig. 4). Since the numerical aperture (NA) of silica and ZrF<sub>4</sub> fibres is 0.22 the optical front end is designed with an F/2 aperture. The inner and the outer target are observed through apertures of about 4 cm diameters with large aspherical mirrors. Two intermediate flat mirrors and a flat combining mirror unite the two optical branches looking at inner and outer target onto a Cassegrain telescope that forms an intermediate image at the divertor exit (= fibre connector). Normal fibres (NA=0.22) illuminate the Cassegrain centrally which has a 30% blind spot in the centre. Hollow fibres (NA=0.05) look at it eccentrically avoiding the blind spot. The mirror design protrudes only very little into the private flux volume above the divertor liner bars – a useful feature should the dome be removed - but demands modifications to 2 of the 4 liners in consequence to the large mirror sizes. The optical resolution of the design is about 3 mm on the targets which corresponds to the ITER requirements. About 500 fibres are necessary to exploit this fully. Experience from Tore Supra [11] shows that the gaps between tiles fill up with deposits which renders them useless for power determination. Looking only at the centre of the tiles (20 mm pitch) reduces the number of fibres to 100. The mirrors (and their box) and the fibres should be cooled. Heated shutters would be useful for calibration and protection.. The

connector at the cassette or the end of the optical relay should be a retractable, replaceable multi-fibre type. The minimum fibre length outside the bioshield is estimated to be 3 m.

A detection system similar to the existing Tore Supra multi-fibre sapphire prism spectrometer [12] coupled to a focal plane array InSb IR camera is a viable detection solution for such a system. Based on the noise levels of the Tore Supra system we expect that the amount of light on the detectors is sufficient to full-fill the most stringent ITER requirements in terms of temporal resolution and low signal level. Fig. 5 illustrates a ( $T_e \leq 2\text{eV}$ ,  $n_e \leq 10^{22}\text{m}^{-3}$ ) case-study where the noise level of a F/6 (as at Tore Supra) detection system (blue line) and of a F/10 and a F/2.5 system (red circles) are compared with the total spectral radiation, the thermal stray-light from within the fibres and the bremsstrahlung from the plasma. In such conditions, the bremsstrahlung limits the detection capabilities at short wavelengths and the thermal stray-light at long wavelengths. The best wavelength range is 2 - 6  $\mu\text{m}$ . Cherenkov radiation in the fibres is expected to be negligible on that scale.

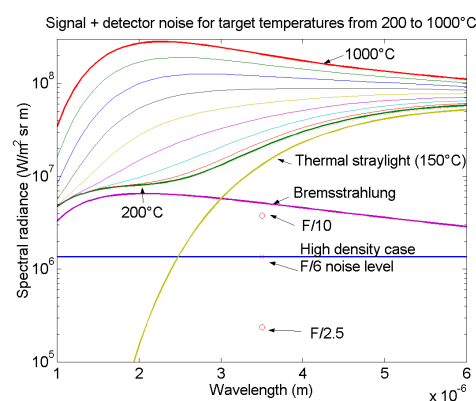


Fig. 5: Performance analysis.

This proposal is based on a spectrally resolved thermography approach which is considered necessary. Optical fibres are a natural choice for such a system and may be implemented to answer sufficiently to the ITER requirements. The optical front end could serve e.g. also for imaging applications if the optical relay would be taken up to the bioshield. In that case the image could provide redundancy to the fibre measurements. A logical next step is to perform radiation tests of true IR fibres.

This work, supported by the European Communities under the contract of Association between EURATOM/CEA-Cadarache, was carried out within the framework of the European Fusion Development Agreement under EFDA contract 02-1003. The views and opinions expressed herein do not necessarily reflect those of the European Commission.

- [1] R. Reichle et al., J. Nucl. Mater., 290-293 (2001) 701-705
- [2] E. Delchambre et al., Journ. Nucl. Mat 337-339 (2005) 1069-1072
- [3] D. Hildebrand, et al., Journ. Nucl. Mat 337-339 (2005)
- [4] K. Itami et al., Rev. Sci. Instr. 75,10 (2004), 4124
- [5] D. Hernandez et al., Rev. Sci. Instr. 76, 024904 (2005)
- [6] T. Loarer and JJ Greffet, Applied optics, Vol.31, N°. 25, (1992), 5350-5358.
- [7] J. A Harington, United States Patent, Number 5,815,627 Date: Sep 29 1998.
- [8] Nuclear Analysis Report, H. Iida, V. Khripunov, L. Petrizzi, Nuclear Analysis Group, ITER Garching Joint Work Site, NAG-201-01-06-17-FDR, G 73 DDD201-06-06 W0.1
- [9] T. Kakuta, T. Shikama, JAERI Research report 2002-007, 34
- [10] B. Brichard, European Fusion Technology Programme Report EUR CIEMAT 93 (2001), 25 and Annexe 6
- [11] R. Mitteau et al., Physica Scripta T111 (2004) 157
- [12] R. Reichle et al., Rev. Sci. Instr. 75,10 (2004), 4129